SIMULATION OF ELECTROMAGNETIC DIFFRACTION WITH TISSUE SCATERING FOR HIGH NUMERICAL-APERTURE OPTICAL SYSTEMS

A Thesis

Presented to the Faculty of the Graduate School

of Cornell University

In Partial Fulfillment of the Requirements for the Degree of

Master of Science

by

Siyan Guo

August 2015

ABSTRACT

In this thesis we discuss the propagation of light with low numerical aperture and high numerical aperture objectives, with or without scattering media. The point spread function (PSF) of a focused beam is studied for low and high aperture situations without scattering medium. Based on the result of other group's Monte Carlo Simulation in treating focus of light in scattering tissue, a simple model has been used to describe and explain the cause of the result. The beams formed by objective lenses with different numerical aperture (NA) are discussed so we can study the influence of changing NA on the focal spot size.

BIOGRAPHICAL SKETCH

Siyan Guo was born in February 16, 1990 in Xi'an, Shaanxi, China. She graduated from the Middle School attached to Northwestern Polytechnical University in Xi'an in 2008. She then attended Fudan University for four years in Shanghai, China and graduated with a major in Physics. After that Siyan attended Cornell University as an MS candidate with a major in Applied Physics. At Cornell she was mainly focused on studying the simulation of tissue scattering. After that she will pursue another master degree in UCR with a major in Statistics. This will help her to study more about the statistical methods.

ACKNOWLEDGMENTS

First, I would like to thank Prof. Xu for his support as my advisor. I am very grateful to him for finding this promising project. He spent a lot of time teaching me knowledge in this field. I really appreciate his patience while helping me and inspiring discussion with me.

Second, I want to thank Prof. Steven Jacques from Oregon Health & Science University, Prof. Min Xu from Fairfield University, and Dr. Fuhong Cai from Zhejiang Univeristy. I really appreciate their patience for discussions with me about their excellent works.

Third, I would like to thank David Sinefeld, Adam Sraub, Tianyu Wang, Rojo Tomas and Li-Chung Cheng. They discussed with me and help me solve problems through my project.

Last, I would like to thank my parents, my boyfriend Yi, my fluffy friend Snickers, and all of my friends. They gave me support and companion through my whole studying-aboard-time.

Contents

1. Introduction

The development of optical imaging is quite popular in biological research and clinical diagnosis, especially deep tissue imaging, which is a new but important field in the medical area. For most imaging methods, resolution is always a key goal for innovation. However, in deep tissue imaging, the existence of absorption and scattering of tissue cause great problems for image focus, resulting in low resolution images. More and more scientists have been working on imaging methods to improve resolution. A new method, laser scanning multi-photon microscopy (MPM), has been invented for solving this problem. Two-photon microscopy is the simplest model for MPM. Two-photon microscopy was invented by Winfried Denk in the lab of Watt W. Webb at Cornell University in 1990, who combined the idea of two-photon absorption with the use of a laser scanner (Winfried Denk, James H. Strckler, Watt W. Webb, 1990). MPM has greatly improved the penetration depth of optical imaging. And now it is a great tool for a variety of deep imaging applications such as intact or semi-intact tissues. (Guanghao Zhu, James van Howe, Michael Durst, Warren Zipfel, and Chris Xu, 2005) However, new concepts and techniques need to be developed for imaging deep into scattering biological tissue.

Since the experimental methods have been well developed for deep-tissue imaging, the theoretical explanation and analytical expressions have not been worked out in this field. The propagation of light has been explained in detail (Wolf, Electromagnetic diffraction in optical systems: I. An integral representation of the image field, 1959), expressing the electrical vector field in low and high numerical aperture (Wolf, Electromagnetic diffraction in optical systems II. Structure of the image field in an aplanatic system, 1959). This paper has explained the most basic and well-developed theory in light propagation. However, this theory cannot explain deep tissue imaging since scattering and absorption have not been considered. No completed theory is

developed for the propagation of light with scattering. So currently, the only way to obtain the analytical result for deep tissue imaging is through numerical simulation. A lot of scientists have developed simulation methods for tissue imaging. For example, Min Xu, an associate professor in Fairfield University, has developed a method called Electric-field Monte Carlo (EMC) Simulation for polarized light propagation in turbid media (Xu, 2004). EMC is a simulation method for tracing the electric field vector of the propagation of light in tissue. Other scientists have combined this method with the specific wavelength range of input light (Fuhong Cai, Jiaxin Yu, Sailing He, 2013). Lihong Wang from Texas A&M and Steven L. Jacques from Oregon Health & Science University, have developed many Monte Carlo simulation methods together, with one example being Monte Carlo For Multi-layered Media (MCML) (Lihong Wang, Steven L. Jacques. Liqiong Zheng, 1995). MCML is a simulation method for tracing the properties of photons such as the position and direction before and after each step for propagation.

The thesis is arranged as follow: Firstly, Electromagnetic diffraction in optical systems for low numerical aperture and high numerical aperture is presented. Secondly, scattering theory is introduced. Thirdly, light propagation in optical systems with low and high numerical aperture objective without scattering medium is investigated. Last, a simple model is shown to explain the result of the Monte Carlo Simulation in treating focusing of light in scattering tissue.

2. Electromagnetic diffraction in optical systems for low numerical aperture

Different diffraction theories can be used to express the phenomena of diffraction qualitatively and quantitatively. For certain aperture, different approximations would be used based on

different field boundaries. This section will explain the vector expression of electromagnetic field diffraction.

(1)Mathematical expressions of diffraction theory

Huygens-Fresnel principle is a common principle of diffraction, which tells that a wave front at a later time is given by the superposition of spherical wavelets originating from a wave front at an earlier time (Gu, 2000). According to the Huygens-Fresnel principle, the diffraction patterns of light propagation can be derived as an integration of the contribution from wavelets of a certain aperture. Consider a small area dS within an aperture, centered at a point P_1. With dS set to be infinitesimal, the total amplitude of waves at P_2 in observation plane can be written as Eq. 1:

$$U(\mathrm{P}_2) = C\iint_{\Sigma} \frac{\exp(-ikr)}{r} U(\mathrm{P}_1)dS \tag{1}$$

Where $U(P_1)$, $U(P_2)$ are the strengths of the illumination at point P_1 and point P_2, respectively.

(2)Kirchhoff Diffraction Theory

Firstly, we consider the scalar condition for this theory. With the field of a monochromatic beam of light expressed with the strength of illumination and time, we could derive Helmholtz equation from Maxwell's equations:

$$(\nabla^2 + k^2)U(\mathrm{P}) = 0 \tag{2}$$

Where

$$\nabla^2 = \frac{\partial^2}{\partial x^2} + \frac{\partial^2}{\partial y^2} + \frac{\partial^2}{\partial z^2} \tag{3}$$

$$k = \frac{2\pi}{\lambda} = \frac{2\pi\, fn}{c} \tag{4}$$

Solving this equation, we could get a rigorous solution

$$U(\mathrm{P}) = \frac{1}{4\pi}\iint_{s}\left[U\frac{\partial}{\partial n}\left(\frac{\exp(-ikr)}{r}\right) - \frac{\exp(-ikr)}{r}\frac{\partial U}{\partial n}\right]dS \tag{5}$$

To get an expression for U(P), several assumptions are needed for evaluation. Krichhoff boundary conditions provide these two assumptions (Gu, 2000): the first one is to show that the field within the aperture is the same as if the screen were absent; the second one is to tell that in other area of the screen, we have

$$\begin{aligned} U &= 0 \\ \frac{\partial U}{\partial n} &= 0 \end{aligned} \tag{6-7}$$

where n is the unit vector of the aperture plane with the same direction of light propagation. By applying these two boundary conditions and using two Green's functions, we could derive the solution to the Helmholtz equations:

$$U_1(P) = -\frac{i}{\lambda}\iint_{\Sigma} U(P_1)\frac{\exp(-ikr)}{r}\cos(\hat{n},\hat{r})\,dS \tag{8}$$

$$U_2(P) = -\frac{1}{2\pi}\iint_{\Sigma}\frac{\partial U(P_1)}{\partial n}\frac{\exp(-ikr)}{r}dS \tag{9}$$

So the equation can be expressed as

$$U_K(P) = \frac{1}{2}\left[U_1(P) + U_2(P)\right] \tag{10}$$

(3) Paraxial Approximation

The light wave propagates close to the axis of the optical components in most diffraction problems, so we need to consider this paraxial approximation in low aperture systems since a lot of other effects will be considered in the high aperture systems.

By applying this approximation, what we need to consider is that the low aperture means the incident angle θ is really small that could result in

$$\begin{aligned} \sin\theta &\approx \theta \\ \tan\theta &\approx \theta \\ \cos\theta &\approx 1 \end{aligned} \tag{11-13}$$

These three assumptions will be used for calculation in low aperture. And in this situation, the input wave can be treated as the plane wave.

3. Electromagnetic diffraction in optical systems for high numerical aperture

(1) Effects of a high numerical-aperture (NA) objective

Since the aperture is no longer low in the system, paraxial approximation is not suitable for this system. Three other effects such as apodization, depolarization and aberration will be considered for the high aperture objective (Gu, 2000).

Apodization shows the difference between the light field distributions over the lens aperture, that is to say, the difference between the distribution of the original input and the distribution of the light passing through the lens or aperture. In low aperture cases, the light distribution over the

lens aperture is almost the same because of the small NA. However, when NA is large, usually larger than 0.7, this difference will become significant. Usually it is to show the difference between a plane wave and a spherical wave.

Depolarization explains that the linearly polarized beam of light will be depolarized in the focus of the lens in a high-aperture system (Gu, 2000). This means the electric field of non-incident direction will be no longer zero.

Aberration shows the changes of the light field in phase over the lens aperture. The high aperture results in complicated aberration function.

(2)Debye Approximation: From Scalar to Vectorial

Debye theory is important in producing a diffraction integral for calculating the diffraction pattern of an objective in high NA system. The spherical surface in Fig.1 can be expressed as

$$U\left(P_1\right) = P\left(P_1\right)\frac{\exp\left(ikf\right)}{f} \tag{14.1}$$

$$U(\mathrm{P}_2) = \frac{i}{\lambda}\iint_{\Sigma} P(\mathrm{P}_1)\frac{\exp\left[-ik\left(r-f\right)\right]}{fr}\cos\left(\vec{n},\vec{r}\right)dS \tag{14.2}$$

Debye approximations contain three parts if P_2 is not far away from the origin: (Using Figure 1 to describe) (Gu, 2000)

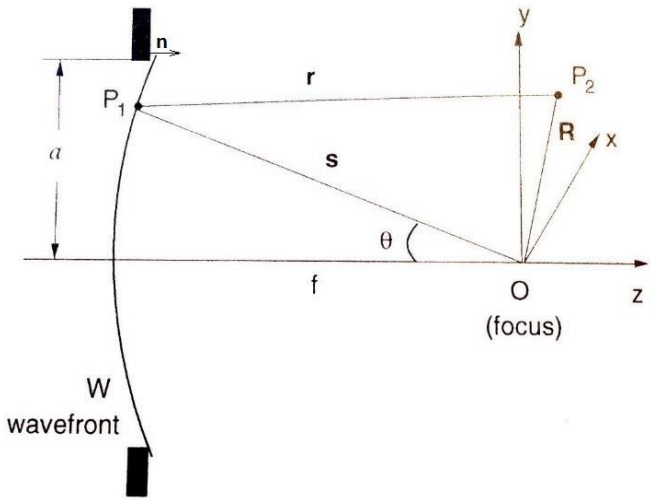

Figure 1.Focusing of a spherical wave

The first approximation shows that the distance difference of $\boldsymbol{r-f}$ can be expressed as cross operating of **s** and **R**. It means the original spherical wavelets can be replaced by a plane wave at the aperture. The second approximation shows that the element area dS can be expressed by the solid angle corresponding to the area dS multiplied by the square of the focal length. The third approximation is that expresses that the direction r is parallel to the optical axis, which means P_1 and P_2 is almost at the same horizontal line, which results to the sine condition: the height along y axis h = fsinθ . To apply these approximations with the original expression of spherical surface U(P) and the result form equation(U_k), we could get the Debye integral

$$U\left(P_2\right)=\frac{i}{\lambda}\iint_{\Omega}P\left(P_1\right)\exp\left(-iks\cdot R\right)d\Omega \tag{15}$$

This is the scalar Debye integral.

In turning to the vectorial situation, we need to use the vectorial wave equation to calculate the electromagnetic field. Firstly we only consider the electric field. By turning the scalar form to vectorial form from equation U(P_2) above, we can get

$$E(P_2) = \frac{i}{\lambda}\iint_{\Omega} E_0(P_1)\exp(-is \bullet R)\, d\Omega \tag{16}$$

To change the coordinate system, for P_1 we use a spherical coordinate system, and for P_2 we use a polar coordinate system. By applying some definite integrals, we could derive from Equation (16) above to

$$E(r_2, \psi, z_2) = \frac{\pi i}{\lambda}\left\{\left[I_0 + \cos(2\psi) I_2\right]\hat{i} + \sin(2\psi) I_2 \hat{j} + 2i\cos\psi I_1 \hat{k}\right\} \tag{17}$$

Where I_0, I_1 and I_2 are (Gu, 2000)

$$\begin{aligned} I_0 &= \int_0^{\alpha} \cos^{1/2}\theta \sin\theta(1+\cos\theta) J_0(kr_2 \sin\theta)\exp(-ikz_2\cos\theta)\, d\theta \\ I_1 &= \int_0^{\alpha} \cos^{1/2}\theta \sin^2\theta J_1(kr_2 \sin\theta)\exp(-ikz_2\cos\theta)\, d\theta \\ I_2 &= \int_0^{\alpha} \cos^{1/2}\theta \sin\theta(1-\cos\theta) J_2(kr_2 \sin\theta)\exp(-ikz_2\cos\theta)\, d\theta \end{aligned} \tag{18-20}$$

4. Scattering Theory

A lot of scattering theories have been developed for describing the scattering of the light by particles. Although these theories have different types of focus, in general they can be divided into two types: single scattering theories, and multiple scattering theories. (Hollis, 2002)

For single scattering, the particles are supposed to be separated largely, or the number of particles are assumed to be small. In other words, compared to the incident wave, the total

scattered wave is small. In that case, the relationship between the incident intensity I and the after-scattered intensity I can be expressed as

$$I = I_0 e^{(\mu_a + \mu_s)l} \tag{21}$$

Where μ_a is the absorption coefficient, and μ_s is the scattering coefficient. l is the transmitted length through the medium.

For multiple scattering, it is no longer focused on one single particle. Instead, it can be treated as the combination of the single scattering, with only the different scattering directions needing to be considered. If the scattering is isotropic, assuming the photons are travelling in a direction $\hat{s}$ into a new direction $\hat{s}'$, by integrating over all the angles, the total scattering coefficient is (Hollis, 2002)

$$\mu_s = \int_{4\pi} d\mu_s(\hat{s}, \hat{s}')\, d\hat{s}' \tag{22}$$

In our study, anisotropic situation is considered for scattering. Here anisotropy factor is introduced to describe our situation

$$g = \int_{4\pi} p(\theta)\cos(\theta)\, d\hat{s}' \tag{23}$$

Where p(θ) is the scattering phase function, which is the normalized version of the differential scattering coefficient. If the scattering is isotropic, g is equal to zero since p is always the same all over different angles. By considering the anisotropic factor, the transport scattering coefficient will be

$$\mu_s' = (1-g)\,\mu_s \tag{24}$$

5. Simulation

(1) Without Scattering

From the expression of electric field of vectoral theory, the intensity is the modulus squared of electric field and can be expressed as (Gu, 2000)

$$I\left(r_2,\psi,z_2\right)=C\left\{\left|I_0\right|^2+4\left|I_1\right|^2\cos^2\psi+\left|I_2\right|^2+2\cos\left(2\psi\right)\mathrm{Re}\left(I_0I_2^*\right)\right\} \tag{25}$$

Where C is the normalization parameter.

When applying the paraxial approximation, that is to say, the maximum angle of convergence of rays in image space, α, is small, we have $J_1(x)\rightarrow 0$ and $J_2(x)\rightarrow 0$ compared with J0(x). So we can get

$$\begin{aligned} &I\left(r_2,\psi,z_2\right)=\left|I_0\right|^2\\ &I_1=0\\ &I_2=0 \end{aligned} \tag{26}$$

That is to say, the intensity is the modulus squared of the variable I_0. So applying paraxial approximation in I_0, we get

$$\begin{aligned} I_0\left(v,u\right)&=\int_0^\alpha\cos^{1/2}\theta\sin\theta\left(\cos^2\frac{\theta}{2}\right)J_0\left(\frac{v\sin\theta}{\sin\alpha}\right)\exp\left(-\frac{1}{2}iu\frac{\sin^2\theta/2}{\sin^2\alpha/2}\right)d\theta\\ &\approx 2\int_0^1 J_0(vx)\exp\left(-1/2\,iux^2\right)xdx\\ &=h\left(v,u\right) \end{aligned} \tag{27}$$

In which

$$v = kr_2 \sin\alpha$$
$$u = 4kz_2 \sin^2\frac{\alpha}{2} \tag{28-30}$$
$$x = \frac{\sin^2\theta/2}{\sin^2\alpha/2}$$

The point spread function PSF is the normalized intensity $I = |I_0|^2 = |h(v,u)|^2$. We have the figure of PSF as Figure 2 (The MATLAB code is in Appendix 1)

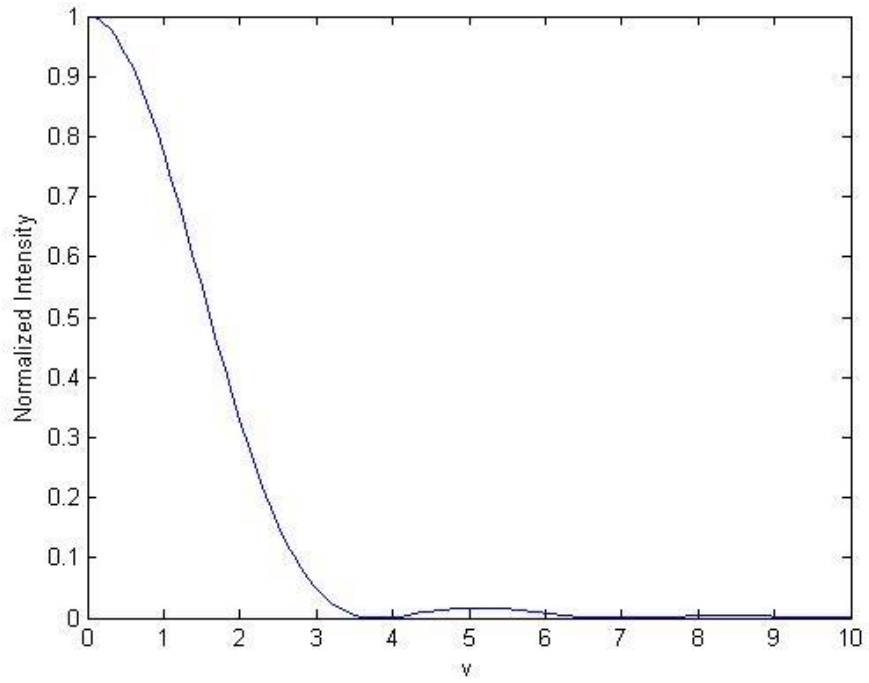

Figure 2. Point Spread Function in low aperture situation

For multi-photon excitation (MPE), under paraxial approximation, a special parameter, a_n, can be defined to determine and distinguish each type of MPE. Let's define the PSF as S(r). The integration of S(r) over the entire volume becomes

$$\int_{V\to\infty} S^n(r)\,dr = a_n C \tag{31}$$

$$a_n = \int_0^\infty 2\pi v dv \int_{-\infty}^{\infty} du \left[h(v,u) \right]^{2n} \tag{32}$$

Here C is a numerical parameter determined by refractive index of media, wavelength of the incident wave and the numerical aperture. This a_n is almost a constant under paraxial approximation over a limited space. n is the number of photon for nPE, for instance, 2-photon excitation is the situation with n = 2. When n = 2, the uncertainty is smaller than 4%, and there is a newly calculated value is $a_n = 64$ when n = 2 (Chris Xu, Watt W. Webb, 1997). A MATLAB code is written to do this calculation (the code is shown in Appendix 1). The result is $a_n = 66.9$, compared with $a_n = 64$, the relative error is 4.5%, a little bit bigger than 4%. That difference may result from the algorithm being used by different people and the uncertainty of the integral boundaries chosen.

When dealing with the high-aperture situation, the paraxial approximation is no longer suitable. That means, the variables I_1 and I_2 no longer approach zero. Therefore we need to consider the Equation (25) when we want to know the PSF in high-aperture situation. In response to this, we developed the MATLAB code (Appendix 2) to get the intensity point spread function normalized at its origin in the two orthogonal directions x axis and y axis, we could get the result that

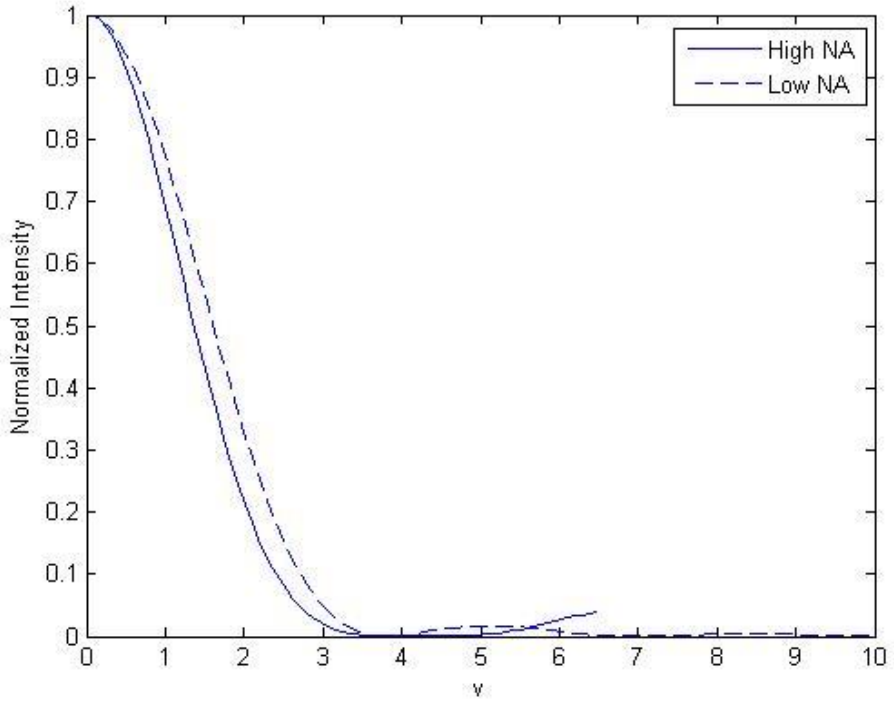

Figure 3.Normalized intensity distribution in a focal region with high aperture objective without scattering. 100 Points are chosen to do the integral. Input wavelength is 1700 nm, and the incident depth is 1mm. The value of NA is 0.87, for the maximum angle of convergence is 60 degree. All scales are in optical unit.

(2) With Scattering

In this project, the absorption coefficient will be considered as zero since it is sufficiently small compared to the scattering coefficient. We have already gotten the result of the in-focus intensity point spread function, so what we need to do is to add the scattering effect into this result to obtain what the situation will be with scattering.

When the light goes into the tissue, the direction of photons will change because of the scattering. A small amount of unscattered photons still exist. That's why the light can still focus through the tissue even though considering the tissue scattering. When the light propagates

through the tissue, the light will be absorbed and scattered, which will cause the intensity of light decrease in the focal plane. At the same time, the focal spot will no longer be that small. Instead, the focal spot will be bigger than before because the incident beam has been scattered through the tissue.

Because the light propagates randomly in the anisotropic tissue, we cannot get the result directly by treating light as wave to determine how the focusing of light will be in the tissue. However, the light can be treated as the large amount of photons incident into the tissue, so we could use Monte Carlo Method to simulate this statistic result. There are many groups using Monte Carlo Method to simulate the propagation of light in the tissue.

A research group in Zhejiang University uses Monte Carlo Method to determine the intensity distribution of a focused laser beam in a tissue (Fuhong Cai, Jiaxin Yu, Sailing He, 2013). A new method, EMC(Electric field Monte Carlo) method has been used in this simulation. EMC simulation is based on tracing the Stocks Vector

$$\vec{I} = \langle I, Q, U, V \rangle^T \tag{33}$$

Where

$$\begin{aligned} I &= \left\langle |E_l|^2 + |E_r|^2 \right\rangle \\ Q &= \left\langle |E_l|^2 - |E_r|^2 \right\rangle \\ U &= \left\langle E_l^* E_r + E_l E_r^* \right\rangle \\ V &= -i \left\langle E_l^* E_r - E_l E_r^* \right\rangle \end{aligned} \tag{34}$$

E_l and E_r are orthogonal compex electri field componets (Xu, 2004). In their simulation, the tissue they use is an aqueous phantom containing 1-um-diameter scattering beads at a

concentration of 0.1044 spheres/micron^3. The main absorption is water and the scattering coefficient is calculated based on Mie scattering theory. For the simulation, they use lasers with different numerical aperture (NA) and get the simulation results for the focal spots. Based on the simulation, it can be concluded that with the increasing of the NA, the focal spot gets smaller. However, as the NA gets larger, the intensity at the focal spot is smaller. In this way, in order to get a better image, we need to figure out a proper NA to make the focal spot small enough, and also bright enough, the result is shown as Fig.4.

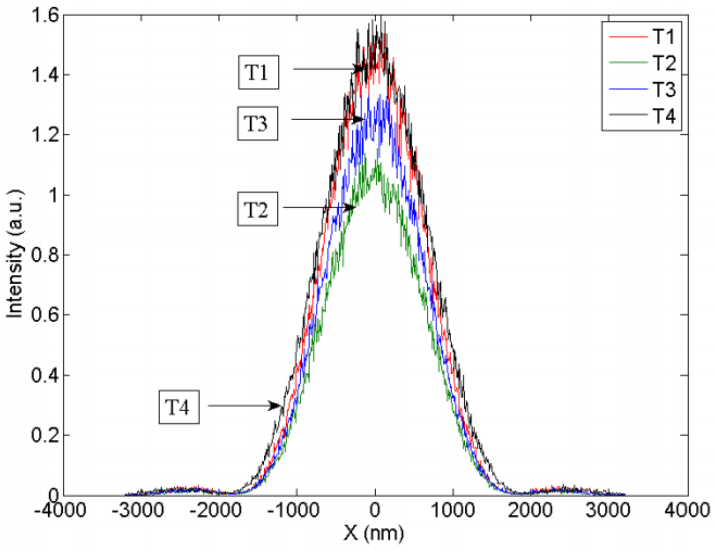

Figure 4 The intensity curves of Focal spots with different NA values (Fuhong Cai, Jiaxin Yu, Sailing He, 2013)

There are a few theories to describe the scattering such as Mie scattering. Here a simple model could be used to describe how scattering could impact the focusing of light in the tissue. Ballistic photons are the photons that travel through a scattering medium in a straight line. When the light propagates through a turbid medium, most of the photons will be randomly scattered or absorbed. So scattering causes photons to depart from their ballistic path. When photons go deep

in the tissue at the focal plane, the probability of scattered photons reaching the focal plane is almost zero. So only ballistic photons can reach the geometrical focus (Ke Wang, Nicholas G. Horton and Chris Xu, 2013). The number of incident photons is assumed the constant in this case, and the surface distribution of photons is uniform. If the NA is larger, the photon density is smaller. With a larger NA, the number of ballistic photons that could reach the center of the focal spot is smaller, so the intensity of the focal spot obtained from the higher NA is smaller. And then, at the focal plane, only ballistic photons will be considered, and the remaining power that they carry falls exponentially with the optical depth $\mu_s z_0$ (A. Leray, C. Odin, E. Huguet, F. Amblard, Y. Le Grand, 2007). The power of ballistic photons with a large incident angle will fall faster because of the longer optical path. So the size of the focal spots obtained from a higher NA objective is smaller.

6. Conclusion

In this project, the simulation of a focused beam propagating without scattering media has been showed. We have obtained the point spread functions without scattering media for both low aperture and high aperture systems. Then, according to the theory of the scattering, we use a simple model to express the impact of scattering on the focus beneath the tissue. We got the result of Sailing He's group, which is, with the increasing of the NA, the focal spot size gets smaller, however, the intensity of the focal spot also decreases. In this way, in order to get a better image, we need to figure out a proper NA to make the focal spot small enough, and also bright enough. More simulations are needed for choosing the NA value.

References

[1] A. Leray, C. Odin, E. Huguet, F. Amblard, Y. Le Grand. (2007). Spaially distributed two-photon excitation fluoresence in scattering media: Experiments and time-resolved Monte Carlo simulations. *Optics Communications*, 269-278.

[2] Chris Xu, Watt W. Webb. (1997). Multiphoton Excitation of Molecular Fluorophores and Nonliar Laser Microscopy. In J. Lakowicz, *Topics in Fluoresecence Spectroscopy; Volume 5: Nonlinear and Two-Photon-Induced Fluresecence* (pp. 471-535). New York: Plenum Press.

[3] Fuhong Cai, Jiaxin Yu, Sailing He. (2013). Vectorial Electric Field Monte Carlo Simulations for Focused laser Beams (800nm-2220nm) in a Biological Sample. *Progress In Electromagnetics Research*, 667-681.

[4] Gu, M. (2000). *Advanced Optical Imaging Theory.* Germany: Springer.

[5] Guanghao Zhu, James van Howe, Michael Durst, Warren Zipfel, and Chris Xu. (2005). Simultaneous spatial and temporal focusing of femtosecond pulses. *Optics Express*, 2153-2159.

[6] Hollis, V. S. (2002). Chapter 2 Light transport in Biological Tissue. In *Non-Invasive Monitoring of Brain Tissue Temperture by Near-Infrared Spectroscopy* (pp. 28-52).

[7] Ke Wang, Nicholas G. Horton and Chris Xu. (2013). Going deep- Brain imaging with multiphoton microscopy. *Optics & Photonics News*, 34-39.

[8] Lihong Wang, Steven L. Jacques. Liqiong Zheng. (1995). MCML- Monte Carlo modeling of light transport in multi-layered tissues. *Computer Methods and Programs in Biomedicine*, 131-146.

[9] Winfried Denk, James H. Strckler, Watt W. Webb. (1990). Two-photon Laser Scanning Fluorescence Microscopy. *Science*, 73-76.

[10] Wolf, E. (1959). Electromagnetic diffraction in optical systems II. Structure of the image field in an aplanatic system. *Proceedings of the Royal Scienty A*, 358-370.

[11] Wolf, E. (1959). Electromagnetic diffraction in optical systems: I. An integral representation of the image field. *Profceedings of the Royal Sciety A*, 349-357.

[12] Xu, M. (2004). Electric field Monte Carlo simulation of polarized light propagation in turbid media. *Optical Express*.

Appendix

1. The code for light propagation without scattering under paraxial approximation (PSF)

```
clear
clc
v = linspace(0,10,101);
dv = 0.1;


PSF = zeros(101);

for i = 1 : 101
    psff = 0;
    for l = 1 : 100
        temp = 0.01*l*besselj(0,v(i)*0.01*l)*dv;
        psff = psff + temp;
    end
    PSF(i) = (abs(2*psff))^2;
end

M = max(PSF);

plot(v,PSF/M)
ylabel('I');
xlabel('v');
```

```
function a = h(v,u,x)
a = x.*besselj(0,v.*x).*exp((-1/2).*1i.*u.*(x)^2);
```

The calculation of a_n when n = 2

```
clear all;
clc;

v = linspace(0,2,100);
u = linspace(-2,2,100);
x =
linspace(0,1,180

 );
```

```
dv = (max(v)-min(v))/(length(v)-1);
du = (max(u)-min(u))/(length(u)-1);
dx = 1/(length(x)-1);
p = 2;
temp = zeros(length(u),length(v),length(x));
for n = 1:length(v)
    n
    for m = 1:length(u)
        for k = 1: length(x)
            temp(m,n,k) =h(v(n),u(m),x(k));
        end
        %hh(m,n) = sum(temp,3);
        %HH(m,n) = (abs(hh(m,n))).^(2*p);

    end
end

hh = sum(temp,3)*dx;
HH = sum(abs(2*hh).^(2*p))*du;

AN = sum(2*pi*HH.*v(n))*dv
```

2. The code for light propagation without scattering in high-aperture system

```
clear,clc
tic
n = 100; % numbers of theta
m = 100; % numbers of r
p = 100; % numbers of z

% unit: um
lamda = 1.7  ;
a = 60*pi/180; % maximum angle of convergence; apeture angle
k = 2*pi/lamda;
phi = pi/2; % along x axis

g = 0.9; % anisotropic factor
miu = 16.67*10^(-3); %scattering coefficient /um

I_zero = zeros(m,p); % # of r rows, # of z column
I_one = zeros(m,p);
I_two = zeros(m,p);
I = zeros(m,p); % total psf
```

```
theta = linspace(0,a,n);
r = linspace(0,0.1,m);
z = linspace(0,1000,p);


for q = 1 : m
   for j = 1 : p
      I_z = 0;
      for k = 1 : n
         temp_z =
sqrt(cos(theta(k))).*sin(theta(k)).*(1+cos(theta(k))).*besselj(0,k.*r(q).*sin(theta(k))).*exp(-
1i*k*z(j).*cos(theta(k)));
         I_z = I_z + temp_z;
      end
      I_zero(q,j) = I_z;
   end
end
%I_zero


for q = 1 : m
   for j = 1 : p
      I_o = 0;
      for k = 1 : n
         temp_o =
sqrt(cos(theta(k))).*((sin(theta(k))).^2).*besselj(1,k.*r(q).*sin(theta(k))).*exp(-
1i*k*z(j).*cos(theta(k)));
         I_o = I_o + temp_o;
      end
      I_one(q,j) = I_o;
   end
end
%I_one

for q = 1 : m
   for j = 1 : p
      I_t = 0;
      for k = 1 : n
         temp_t = sqrt(cos(theta(k))).*sin(theta(k)).*(1-
cos(theta(k))).*besselj(2,k.*r(q).*sin(theta(k))).*exp(-1i*k*z(j).*cos(theta(k)));
         I_t = I_t + temp_t;
      end
      I_two(q,j) = I_t;
   end
end
```

```
%I_two

for q = 1 : m
   for j = 1 : p
      I(q,j) = (abs(I_one(q,j))).^2 + 4*(abs(I_one(q,j))^2)*((cos(phi))^2) + (abs(I_two(q,j)))^2
+ 2*cos(2*phi)*(real(I_one(q,j)*conj(I_two(q,j))));
   end
end
%I

NORM_max = max(I(:,1))
I_norm = I(:,1)/NORM_max;

R = k.*r.*sin(a);

%when u = 0, which means z = 0, we could get the psf is first column, which
%is (:,1)
figure(1)
plot(R,I_norm)

toc
```

LIST OF FIGURES